CMS Draft Analysis Note

2024/10/02
Archive Hash: untracked
Archive Date: 2024/10/02

Differential cross section measurements of single top and $t\bar{t}$ in association with a photon production

Ying An[1], Maria Aldaya[1], Hugo Alberto Becerril Gonzalez[1], Abideh Jafari[2], and Andreas Meyer[1]

[1] DESY, Hamburg, Germany
[2] Isfahan University of Technology, Isfahan, Iran

Abstract

This note presents the study of measuring $t\bar{t}$ and single top in association with a photon simultaneously. Both the inclusive and differential cross sections are measured in proton-proton (pp) collisions at a center-of-mass energy of $\sqrt{s} = 13\,\text{TeV}$, based on the data recorded by the CMS experiment, corresponding to an integrated luminosity of $138\,\text{fb}^{-1}$. Measurements are performed in events with a well-isolated, highly energetic lepton (electron and muon), at least two jets from the hadronization of quarks, and an isolated photon. The photon emitted from initial state radiation, top quark, and top quark decay products, are simulated in separated samples. Differential cross sections as functions of the leading photon transverse momentum, the leading lepton transverse momentum, the number of forward jet transverse momentum, and ΔR of some particles including reconstructed top are presented. The measurement is also carried out differentially in several kinematic observables and interpreted in the context of effective field theories.

1 Introduction

This note presents a simultaneous measurement for productions of $t\bar{t}$ and single top in association with a photon, referred to as $t\bar{t}\gamma$ and $t\gamma q$, using the proton-proton (pp) collisions data at a center-of-mass energy of $\sqrt{s} = 13\,\text{TeV}$, which corresponds to an integrated luminosity of $138\,\text{fb}^{-1}$ and is recorded by the CMS detector. The measurements focus on the single lepton decay channel with final states of exactly one lepton, at least one photon and two jets where at least one jet should be tagged by the b jet tagging discriminant.

Due to the unique feature of the top quark in the fermion family, its properties are studied and measured well covering measurements on the mass, cross sections, charge or energy asymmetry, etc. The relevant top quark productions can be classified into cases of t-channel and s-channel single top productions, $t\bar{t}$ production, tX or $t\bar{t}X$ production (X=W, Z, γ), which are described well by the Standard Model (SM). For the tX and $t\bar{t}X$ productions, they represent a direct probe of the top quark to the gauge bosons couplings that determine the value of cross sections. The precise measurements, especially the differential cross sections, can uncover any deviation to the SM which could indicate a beyond SM (BSM) hint. On the other hand, these productions are usually important backgrounds in other analyses. The differential cross section measurements are hence really useful. Furthermore, the direct top-photon coupling can be as a platform to search for any anomalous couplings.

In this note, the goal is to study the t-γ coupling by measuring the $t\gamma q$ and $t\bar{t}\gamma$ productions simultaneously. Both inclusive and differential cross sections will be measured. Then interpret the results in the context of the SM effective field theory (SMEFT). The $t\gamma q$ process is observed by ATLAS and the inclusive cross section is presented. The $t\bar{t}\gamma$ process is measured both inclusively and differentially by ATLAS and CMS collaborations. In $t\gamma q$ and $t\bar{t}\gamma$ measurements, they are mutual background. A simultaneous fit could help get the full set of correlations between the two processes and provide a straightforward EFT interpretation with more constraints for the same EFT operators. We focus on the single lepton channel where W decays to $\ell\nu$ from $t \to bW$, which is the better decay channel in $t\gamma q$ compared to the fully hadronic channel and a high statistics channel in $t\bar{t}\gamma$. Fig 1 shows the LO Feynman diagrams for $t\gamma q$ and $t\bar{t}\gamma$ productions, where the photon can be either from the production including from the top quark directly and initial quark (ISR) or from the top quark decay products. These two kinds of photons are simulated from separated samples, hence, cross sections for photons from production only or from production plus FSR can be measured respectively.

2 Data and simulation

In this simultaneous $t\bar{t}\gamma + t\gamma q$ measurement, we use the full Run-2 data and simulation in the ultra-legacy (UL) campaign with NANOAOD v9 version.

2.1 Data samples

The data is from the pp collisions at a center-of-mass energy of 13 TeV, corresponding to an integrated luminosity of 138 fb^{-1}, recorded by the CMS detector from 2016 to 2018. Data used in the measurement pass the certifications from different physics detector groups (PDG) and physics object groups (POG) which are recorded in the GOLDEN JSON file. Table 1 shows the GOLDEN JSON files used from 2016 to 2018. Because the cross section is measured in a single-lepton phase space, the "SingleMuon" and "SingleElectron" ("EGamma") datasets are used as shown in Table 2.

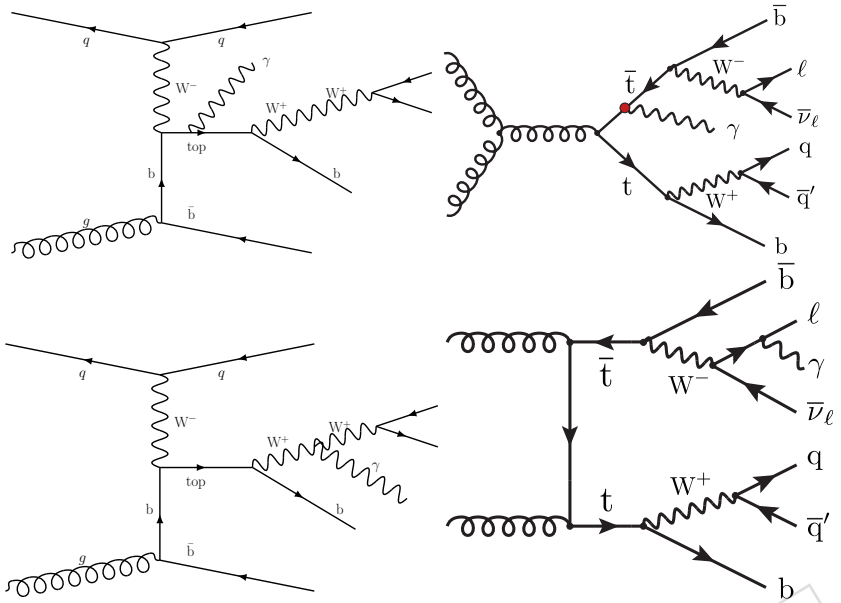

Figure 1: Representative Feynman diagrams for $t\gamma q$ (left column) and $t\bar{t}\gamma$ (right column). The upper row is productions with the direct top and photon coupling. The lower row is productions with the photon radiated from the top quark decay products.

Table 1: Summary of the GOLDEN JSON files for 2016–2018.

Year	GOLDEN JSON file
2016	Cert_271036-284044_13TeV_Legacy2016_Collisions16_JSON.txt
2017	Cert_294927-306462_13TeV_UL2017_Collisions17_GoldenJSON.txt
2018	Cert_314472-325175_13TeV_Legacy2018_Collisions18_JSON.txt

2.2 Simulation

All simulation samples considered in this analysis come from the official version of RunIISummer20UL16NanoAODAPV9 and RunIISummer20UL16NanoAODv9 for 2016, RunIISummer20UL17NanoAODv9 for 2017, and RunIISummer20UL18NanoAODv9 for 2018. The list of all simulations with their cross section values is shown in Table **??**.

We have several CMS official samples to simulate the processes of $t\bar{t}\gamma$ and $t\gamma q$, especially for $t\bar{t}\gamma$, there are two kinds of simulations with and without the FSR photon taken into account.

For the $t\gamma q$ process, we only have the simulation that only includes matrix-element photon. It's generated by the MADGRAPH5_aMC@NLO (MG5) with the default version 2.6.5 at next-to-leading (NLO) in quantum chromodynamics (QCD) accuracy. The full syntax from the MG5 is as the expression 1, where the mark "\$\$ W^+ W^-" means to forbid any $W^\pm$ in s-channel which has little and negligible effect to the final cross section value. A cross-check is done by generating process with or without "\$\$ W^+ W^-" using syntax *generate* $pp \rightarrow t\ \bar{b}\ j\ \gamma$ and

Dataset stream	Era	luminosity [fb^{-1}]
SingleMuon (SingleElectron)	Run2016B-ver2_HIPM_UL2016_MiniAODv2_NanoAODv9-v2 Run2016B-ver1_HIPM_UL2016_MiniAODv2_NanoAODv9-v2 Run2016C-HIPM_UL2016_MiniAODv2_NanoAODv9-v4 Run2016D-HIPM_UL2016_MiniAODv2_NanoAODv9-v2 Run2016E-HIPM_UL2016_MiniAODv2_NanoAODv9-v2 Run2016F-HIPM_UL2016_MiniAODv2_NanoAODv9-v2	19.4
	Run2016F-UL2016_MiniAODv2_NanoAODv9-v1 Run2016G-UL2016_MiniAODv2_NanoAODv9-v2 Run2016H-UL2016_MiniAODv2_NanoAODv9-v1	16.8
SingleMuon (SingleElectron)	Run2017B-UL2017_MiniAODv2_NanoAODv9-v1 Run2017C-UL2017_MiniAODv2_NanoAODv9-v1 Run2017D-UL2017_MiniAODv2_NanoAODv9-v1 Run2017E-UL2017_MiniAODv2_NanoAODv9-v1 Run2017F-UL2017_MiniAODv2_NanoAODv9-v1	41.52
SingleMuon (EGamma)	Run2018A-UL2018_MiniAODv2_NanoAODv9-v1 Run2018B-UL2018_MiniAODv2_NanoAODv9-v1 Run2018C-UL2018_MiniAODv2_NanoAODv9-v1 Run2018D-UL2018_MiniAODv2_NanoAODv9-v3	59.8

Table 2: List of reconstructed data samples used in the analysis. The NANOAOD v9 format is used.

generate $pp \to \mathrm{t}\,\bar{\mathrm{b}}\,\mathrm{j}\,\gamma$ \$\$ $\mathrm{W}^+\,\mathrm{W}^-$, which corresponding to cross sections 0.272 and 0.271 fb.

$$\textit{generate } pp \to \mathrm{t}\,\bar{\mathrm{b}}\,\mathrm{j}\,\gamma\ \$\$\ \mathrm{W}^+\,\mathrm{W}^-\ [\mathrm{QCD}] \tag{1a}$$

$$\textit{add process } pp \to \bar{\mathrm{t}}\,\mathrm{b}\,\mathrm{j}\,\gamma\ \$\$\ \mathrm{W}^+\,\mathrm{W}^-\ [\mathrm{QCD}] \tag{1b}$$

$$\begin{aligned}\text{MadSpincard}: \quad & \textit{decay } \mathrm{t} \to \mathrm{W}^+\,\mathrm{b},\ \mathrm{W}^+ \to \ell^+\nu \\ & \textit{decay } \bar{\mathrm{t}} \to \mathrm{W}^-\,\bar{\mathrm{b}},\ \mathrm{W}^- \to \ell^-\bar{\nu}\end{aligned} \tag{1c}$$

The FSR photon contribution in the $\mathrm{t}\gamma\mathrm{q}$ process, referred to as $\mathrm{t}(\to \ell\nu\mathrm{b}\gamma)\mathrm{q}$, can be added from the single t t-channel production after an overlap removal with the above $\mathrm{t}\gamma\mathrm{q}$ simulation. The details of the procedure in overlap removal are introduced in Section 2.3.

In the generator-level with requirements in our fiducial region shown in Table **??** and overlap removal between $\mathrm{t}\gamma\mathrm{q}$ and single t t-channel productions, several distributions extracted by the 2018 simulations are shown in Figure 2. The cases in 2016 and 2017 are almost the same. From these plots, we can get the conclusion that the $\mathrm{t}(\to \ell\nu\mathrm{b}\gamma)\mathrm{q}$ contribution shows an obvious shape effect in p_{T}^{γ} and $\Delta R(\ell,\gamma)$ distributions and a normalization effect in the N_{jets} distribution. The amount of the $\mathrm{t}(\to \ell\nu\mathrm{b}\gamma)\mathrm{q}$ contribution accounts for around 20% which is mainly from the low p_{T}^{γ} and $\Delta R(\ell,\gamma)$ and becomes negligible when $p_{\mathrm{T}}^{\gamma} > 50\,\mathrm{GeV}$. The list of simulation samples for extracting the Figure 2 is shown in Table 3.

For the $\mathrm{t}\bar{\mathrm{t}}\gamma$ process, we have two kinds of simulations. One is with the same setting as the $\mathrm{t}\gamma\mathrm{q}$ simulation that only has the matrix-element photon, referred to as NLO $\mathrm{t}\bar{\mathrm{t}}\gamma$, generated by the MADGRAPH5_aMC@NLO (MG5) at NLO in QCD accuracy with a MadSpind card to decay t in single-lepton phase space. The other is generated by the MADGRAPH5_aMC@NLO (MG5) at LO but includes both matrix-element and FSR photons with syntax as the expression 2, referred to

Process	Sample	XS (pb)
$t\gamma q$	TGJets_leptonDecays_TuneCP5_13TeV-amcatnlo-pythia8	0.995
$t(\rightarrow \ell\nu b\gamma)q$	ST_t-channel_top_4f_InclusiveDecays_TuneCP5_13TeV-powheg-madspin-pythia8	136
	ST_t-channel_antitop_4f_InclusiveDecays_TuneCP5_13TeV-powheg-madspin-pythia8	80.95

Table 3: List of simulation samples for extracting matrix-element and FSR photons in the $t\gamma q$ process.

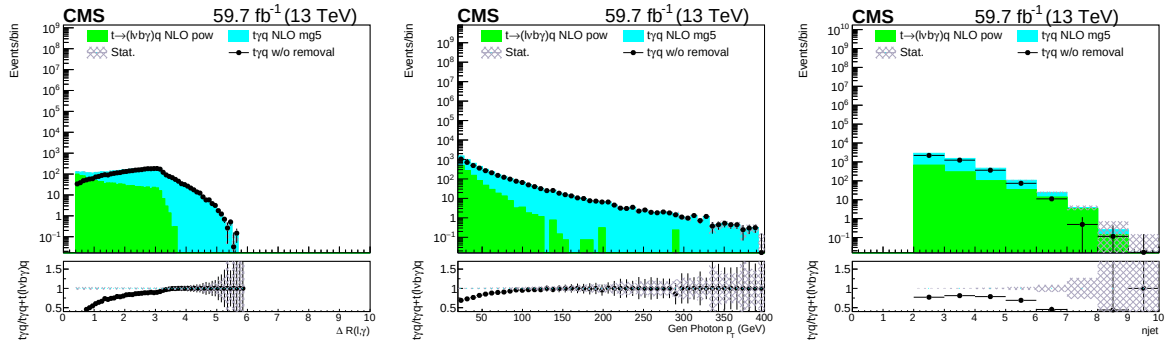

Figure 2: Contributions of $t\gamma q$ (green) and $t(\rightarrow \ell\nu b\gamma)q$ (cyan) after overlap removal between $t\gamma q$ and single t t-channel samples. The data points are contributions from $t\gamma q$ simulation without overlap removal application.

as LO $t\bar{t}\gamma$.

$$generate\ pp \rightarrow t\,\bar{t}\ \rightarrow \ell^{+}\nu\ b\ jj\ \bar{b}\ \gamma \tag{2a}$$

$$add\ process\ pp \rightarrow t\,\bar{t}\ \rightarrow jj\ b\ \ell^{-}\bar{\nu}\ \bar{b}\ \gamma \tag{2b}$$

Besides obtaining FSR photon contribution in $t\bar{t}\gamma$ process from the LO $t\bar{t}\gamma$ simulation, we could also estimate it from the $t\bar{t}$ + jets samples with the overlap removal applied. It's also possible to compare the contribution between LO $t\bar{t}\gamma$ and NLO $t\bar{t}\gamma$ plus $t\bar{t}$ + jets. The former has a complete photon contribution but a normalisation factor is needed because it's an LO sample. The latter is the sum of matrix-element photon and FSR photon if the overlap removal is applied, which should be comparable to the normalized LO $t\bar{t}\gamma$ contribution. Figure 3 shows some distributions from 2018 simulations for this comparison in our fiducial region shown in Table **??**. The cases in 2016 and 2017 are almost the same. The list of simulation samples for extracting Figure 3 is shown in Table 4. We finally find that in our fiducial region, a k-factor of 1.86 should be applied to the LO $t\bar{t}\gamma$ production. From the N_{jets} distribution, we can observe a reduction effect in LO $t\bar{t}\gamma$ sample with the number of jets increasing, which is reasonable, because the LO simulation can't model multi-jets well. This also prompts us to use the NLO $t\bar{t}\gamma$ sample as the signal sample for the $t\bar{t}\gamma$ process.

For the $t\bar{t}$ + jets production, there are samples generated by MADGRAPH5_aMC@NLO and POWHEG and are both with NLO QCD correction. The different generator doesn't affect the FSR photon contribution as shown in Figure 4 with the signal region requirement at the reconstruction-level, where only MC statistical uncertainties are included. Within uncertainties, they agree with each other.

Process	Sample	XS (pb)
NLO $t\bar{t}\gamma$	TTGJets_TuneCP5_13TeV-amcatnloFXFX-madspin-pythia8	2.967
LO $t\bar{t}\gamma$	TTGamma_SingleLept_TuneCP5_13TeV-madgraph-pythia8	5.056
	TTGamma_Dilept_TuneCP5_13TeV-madgraph-pythia8	1.495
$t\bar{t}$ + jets	TTToSemiLeptonic_TuneCP5_13TeV-powheg-pythia8	367.85
	TTTo2L2Nu_TuneCP5_13TeV-powheg-pythia8	89.28
	TTJets_TuneCP5_13TeV-amcatnloFXFX-pythia8	833.9

Table 4: List of simulation samples for extracting matrix-element and FSR photons in the $t\bar{t}\gamma$ process.

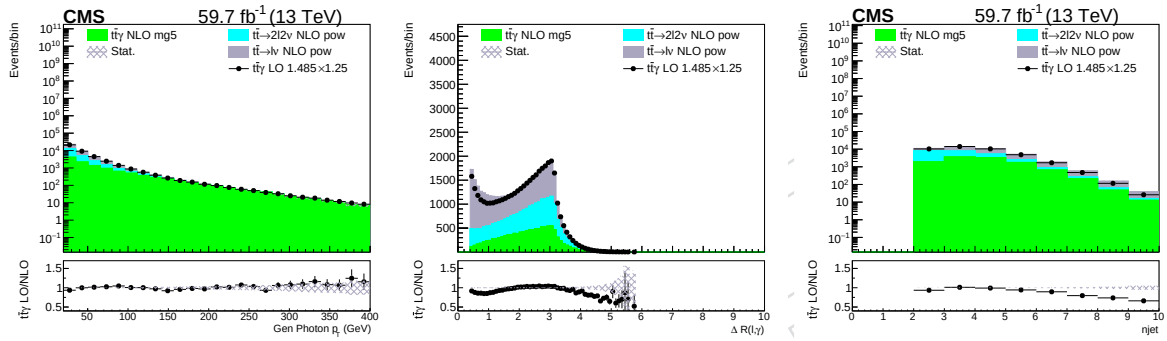

Figure 3: Contributions of $t\bar{t}\gamma$ (green) and $t\bar{t} \to \ell\nu bjj\bar{b}\gamma$ (cyan and grey) after overlap removal between NLO $t\bar{t}\gamma$ and $t\bar{t}$ + jets samples. The data points are contributions from a normalized LO $t\bar{t}\gamma$ simulation without overlap removal application.

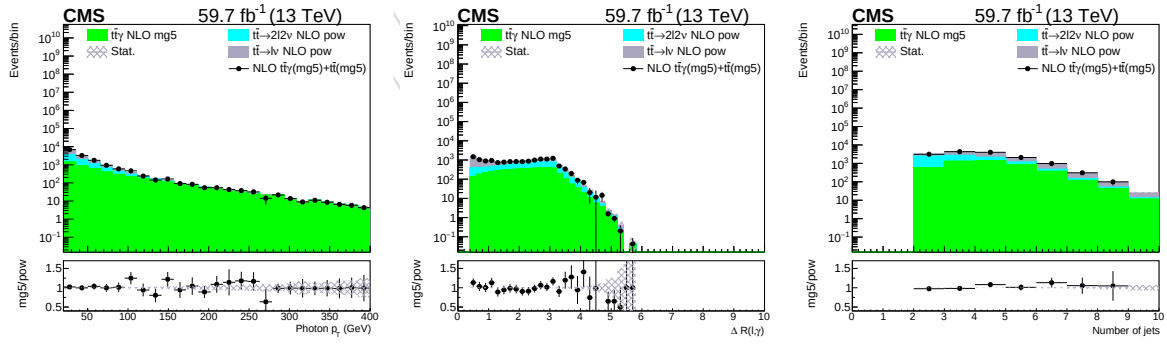

Figure 4: Contributions of $t\bar{t}\gamma$ and $t\bar{t} \to \ell\nu bjj\bar{b}\gamma$ (cyan and grey) after overlap removal between NLO $t\bar{t}\gamma$ and $t\bar{t}$ + jets MG5 (data points) or POWHEG (filled histogram) samples. The data points are the sum of the matrix-element photons from the NLO $t\bar{t}\gamma$ and FSR photons from the MG5 $t\bar{t}$ + jets.

2.3 Overlap removal

Separate samples are used for the $t\gamma q$ ($t\bar{t}\gamma$) and the single t t-channel ($t\bar{t}$ + jets) productions. The the single t t-channel ($t\bar{t}$ + jets) sample contains events where a shower photon is radiated at high energy and at a large angle. This phase space could be also covered by the $t\gamma q$ ($t\bar{t}\gamma$)

sample and thus the overlap must be removed by vetoing events in the single t t-channel ($t\bar{t}$ + jets) sample that fall into the $t\gamma q$ ($t\bar{t}\gamma$) phase space. The case also suits processes of $Z\gamma$ and Z + jets, $W\gamma$ and W + jets, etc, referred to as $X\gamma$ and X+jets.

We can make use of generator-level information to avoid the overlap between these samples. A good generator-photon can be defined and it should pass some strict requirements to qualify it's similar to a matrix-element photon from $X\gamma$ sample as much as possible. Next, we require the $X\gamma$ sample to contain at least one such generator-photon, and the X+jets events are required not to fall into the region containing such generator-photon. So the overlap is removed between these samples. The requirements of such a good generator-photon are summarized in Table 5, where `isPrompt` means the photon not from hadron, μ or τ decay, and the ΔR cone size is defined according to the value of `R0gamma` used in their MG5 "run_card.dat". Within the ΔR cone size, we impose the good generator-photon should be isolated with other generator-particles, where these generator-particles should satisfy $p_{\mathrm{T}}^{\mathrm{gen}} > 5\,\mathrm{GeV}$, `status` $= 1$, and not neutrinos and the generator-photon itself. In MG5 run_card.dat, `R0gamma` is the radius of isolation between photons and quarks/gluons. A smaller value of `R0gamma` for an NLO process with a photon in the final state affects the emission of the additional jets and is able to include the additional jets more inclusively.

Selection/Process	$t\gamma q$/single t t-channel	$t\bar{t}\gamma/t\bar{t}$ + jets	$Z\gamma/Z$ + jets	$W\gamma/W$ + jets
|`pdgId`|		22		
`status`		$1 \rightarrow$ stable particle		
`Mother`	from top or ISR	from top or ISR	`isPrompt`	`isPrompt`
p_{T}^{γ} (gen)		$> 20\,\mathrm{GeV}$		
$\lvert\eta^{\gamma}\rvert$ (gen)		< 2.5		
ΔR cone size	0.05	0.05	0.05	0.05

Table 5: List of requirements to define a good generator-photon for overlap removal between $X\gamma$ and X+jets.

Figure 5 and 6 show the comparison of $X\gamma$ and X+jets before and after the overlap removal in distributions of p_{T}^{γ} and $\Delta R(\ell, \gamma)$. These plots meet the requirement of exactly one good lepton and at least one good photon at the reconstruction level, details of the good lepton and photon are described in Section 3. We can find that if the $X\gamma$ is simulated in such completed phase space, such as the LO $t\bar{t}\gamma$, after the overlap removal application, the X+jets only remains very few contributions like central and right plots in the upper row of the Figure 5 and 6. But if the $X\gamma$ lacks a dedicated production mode, for example, the NLO $t\bar{t}\gamma$ lacks the FSR photons, then after the overlap removal application, the X+jets remains quite a lot contribution as the left plot in the lower row of the Figure 5 and 6 shown.

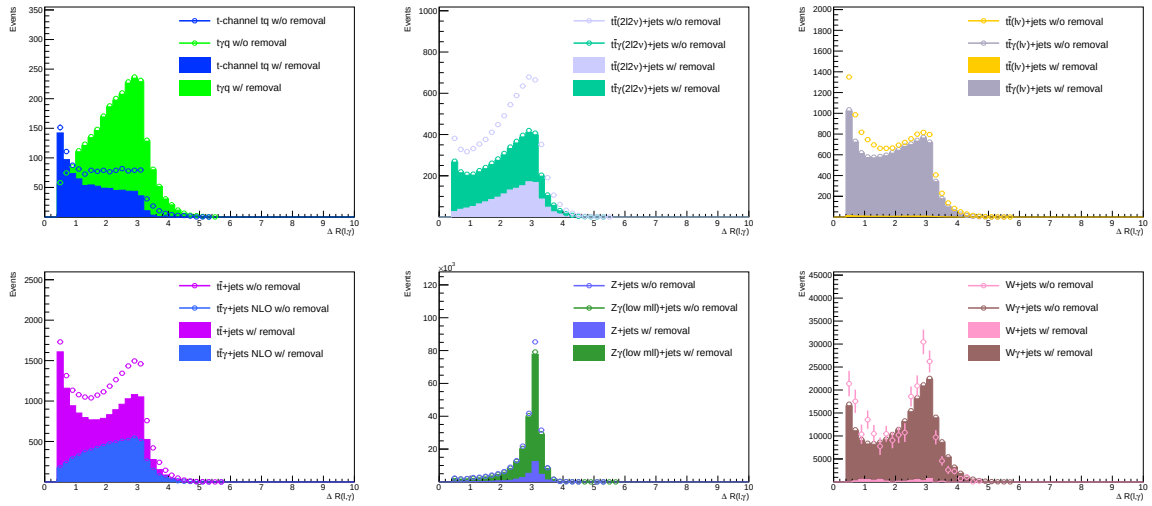

Figure 5: Contributions of Xγ and X+jets before (circle) and after (filled histograms) overlap removal in distributions of $\Delta R(\ell, \gamma)$.

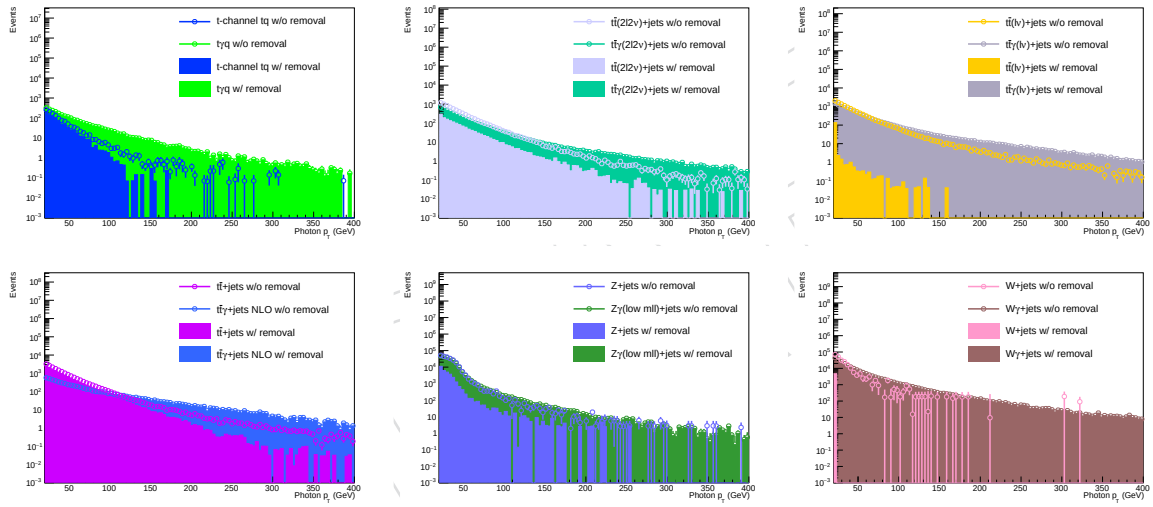

Figure 6: Contributions of Xγ and X+jets before (circle) and after (filled histograms) overlap removal in distributions of p_{T}^{γ}.